Article ID: 1671-3664(2005)02-0201-12

Identification of acceleration pulses in near-fault ground motion using the EMD method

Zhang Yushan (张郁山)[1†], Hu Yuxian (胡聿贤)[2‡], Zhao Fengxin (赵凤新)[2‡], Liang Jianwen (梁建文)[1‡] and Yang Caihong (杨彩红)[1§]

1. *Department of Civil Engineering, Tianjin University, Tianjin 300072, China*
2. *Institute of Geophysics, China Earthquake Administration, Beijing 100081, China*

Abstract: In this paper, response spectral characteristics of one-, two-, and three-lobe sinusoidal acceleration pulses are investigated, and some of their basic properties are derived. Furthermore, the empirical mode decomposition (EMD) method is utilized as an adaptive filter to decompose the near-fault pulse-like ground motions, which were recorded during the September 20, 1999, Chi-Chi earthquake. These ground motions contain distinct velocity pulses, and were decomposed into high-frequency (HF) and low-frequency (LF) components, from which the corresponding HF acceleration pulse (if existing) and LF acceleration pulse could be easily identified and detected. Finally, the identified acceleration pulses are modeled by simplified sinusoidal approximations, whose dynamic behaviors are compared to those of the original acceleration pulses as well as to those of the original HF and LF acceleration components in the context of elastic response spectra. It was demonstrated that it is just the acceleration pulses contained in the near-fault pulse-like ground motion that fundamentally dominate the special impulsive dynamic behaviors of such motion in an engineering sense. The motion thus has a greater potential to cause severe damage than the far-field ground motions, i.e. they impose high base shear demands on engineering structures as well as placing very high deformation demands on long-period structures.

Keywords: acceleration pulse; velocity pulse; near-fault pulse-like ground motion; empirical mode decomposition (EMD); response spectrum

1 Introduction

Near-fault ground motions affected by forward directivity or fling step usually contain distinct pulses in their waveforms (Aki, 1968; Archuleta and Hartzell, 1981; Bolt, 1983). It has been demonstrated that such pulses are more prominent in the velocity or displacement time histories than in the acceleration histories (Singh, 1985). Due to their unique impulsive nature, as well as their potential to cause severe damage to structures, the near-fault pulse-like ground motions have been comprehensively studied in the seismological and earthquake engineering communities (e.g., Iwan, 1997; Malhotra, 1999; Chopra and Chintanapakdee, 2001; Mavroedis *et al*., 2004 among numerous others). Low-frequency velocity pulses have been the focus of most of these previous studies and several simple yet effective mathematical models have been proposed for these velocity pulses (Someville, 1998; Alavi and Krawinkler, 2000; Sasani and Bertero, 2000; Makris and Chang, 2000; Agrawal and He, 2002; Mavroedis and Papageorgiou, 2003). This is due to two main reasons. First, compared with the acceleration pulse, the low-frequency velocity pulse can be easily identified at the beginning of the velocity waveform. Second, and more importantly, parameters involved in simple mathematical models for these velocity pulses, such as the amplitude and the duration, have unambiguous physical interpretations and are directly related to seismological parameters such as earthquake magnitude, rise time, and the shortest distance from the site to the source (Somerville *et al*., 1997; Somerville, 1998; Mavroedis and Papageorgiou, 2003; Mavroedis *et al.*, 2004).

Even so, despite the fact that much effort has been invested in the study of near-fault velocity pulses, and some important concepts in earthquake engineering have been advanced from these studies, the engineering implications of acceleration pulses contained in near-fault ground motion has also interested some researchers (Bertero, 1976; Bertero *et al*., 1978; Sucuogly *et al.,* 1999; Makris and Black, 2004), and the dynamic responses of a structure under excitations simulated by several simplified mathematical acceleration pulses have

Correspondence to: Zhang Yushan, Department of Civil Engineering, Tianjin University, Tianjin 300072, China
Tel: 86-22-27404025
E-mail: hyszhang@163.com
†Ph.D. student; ‡Professor; §Graduate Student

Supported by: Natural Science Foundation of China Under Grant No. 50278090
Received 2005-08-30; **Accepted** 2005-11-14

been investigated (Jennings, 2001; Dai *et al*., 2004). Furthermore, regardless of how well the parameters of velocity pulse correlate with the seismological parameters, it is the acceleration history that is used to compute the seismic response of structures and velocity pulse models need to be differentiated to study the structural response. However, sometimes the acceleration waveforms obtained by differentiating some simplified velocity pulses may be totally distorted from the original records (Zhang *et al*., 2003). Thus, identifying the acceleration pulses from near-fault pulse-like seismic records, and further, directly establishing the mathematical models for the acceleration pulses, may have theoretical and practical significance. In general, there may be two types of acceleration pulses contained in the near-fault ground motions, i.e. high-frequency (HF) and low-frequency (LF). The HF acceleration pulse usually has large amplitude and short duration, and can be easily detected from the accelerogram, but it may not contribute very much to the velocity pulse that is often low-frequency predominant. Whereas, the LF acceleration pulse is well-related to the LF velocity pulse, but in the acceleration waveform, the other HF components often ride on this LF pulse, making it less prominent in the acceleration waveform, as mentioned above. Therefore, using a proper data processing technique that separates these two types of acceleration pulses from the original records will identify them and their individual contributions to the damage potential of original ground motion.

By using the empirical mode decomposition (EMD) method, introduced by Huang *et al*. (1998), a given data, such as a seismic record, can be decomposed into a finite number of intrinsic mode functions (IMFs). Further, by grouping the corresponding IMF components according to some prescribed criterion, subjective or objective, the EMD method can be used as an adaptive filter (Zhang *et al*., 2003), making it possible for the HF and LF acceleration pulses to be separated and identified from the original seismogram.

In this paper, the characteristics of response spectra of simplified one-, two- and three-lobe sinusoidal acceleration pulses are studied first. Some basic properties of acceleration pulses are derived. Then, the EMD method is used to decompose the velocity time histories, which were obtained from the 1999 Chi-Chi earthquake and have prominent pulses, into the corresponding velocity IMF components. By grouping the first three IMF components, the HF velocity component can be obtained; while adding the remained IMF components yields the LF velocity component. Differentiating the HF and LF velocity components generates the HF and LF acceleration components that may contain the HF and LF acceleration pulses, respectively. Then, in the context of elastic response spectra, the pulse natures of the HF and LF acceleration components and their contributions to the damage potential of original impulsive ground motion are investigated.

2 Sinusoidal acceleration pulses

The one-, two- and three-lobe sinusoidal models of acceleration pulses are shown in Fig. 1, where their amplitudes are units and their periods are denoted by T_0. According to the ratio of T_0 to the natural vibration period of structure, T, the acceleration pulse can be classified as either fast pulse or slow pulse (Jennings, 2001). If $T >> T_0$, then the acceleration pulse is a fast pulse; otherwise, it is a slow pulse. The spectral accelerations, velocities, and displacements of these acceleration pulses with T_0 being 0.5 s, 1.0 s, and 5.0 s are shown in Fig. 2, where the damping ratio, $\zeta = 0.05$ was taken, and the time durations of all input acceleration time histories are 50.0 s. With the input pulse period, T_0, fixed and the structural natural period, T, varying, in some interval on the abscissa of T of the response spectrum, the input sinusoidal acceleration pulse is regarded as fast pulse, and the associated range of T is defined as a non-resonance band or impulse band accordingly; while in the other interval, it is regarded as slow pulse, and the associated range of T is defined as a resonance band or cyclic band. In the non-resonance band, the input sinusoidal acceleration pulse behaves in a similar way as the Dirac-delta-type impulse load, as there is almost no time for resonance to build-up, and it is the area under the pulse, instead of the details of the pulse shape, that has a major effect on the response of a structure. In the resonance band, the input sinusoidal acceleration pulse is like the cyclic load, which has some time for resonance to build-up, and the pulse details have an effect on the structural response. In Fig.2, for one fixed value of T_0, the interval of $0.0 \text{ s} \le T \le 3T_0$ is approximately regarded as the resonance band, while the interval of $T > 3T_0$ is non-resonance band. When $T_0 = 5.0$ s, the non-resonance band is beyond the normal natural period range of $0.0 \text{ s} \le T \le 10.0$ s that encompasses a majority of

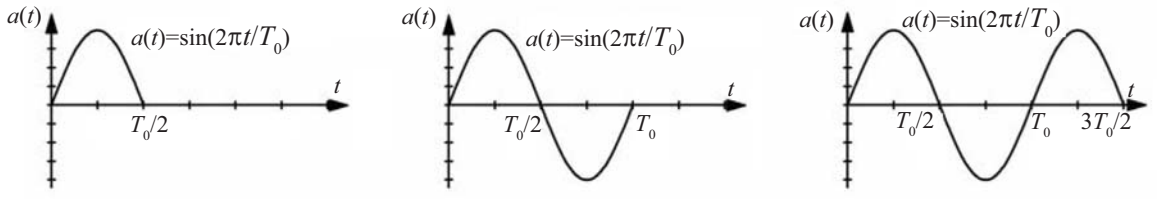

(a) One-lobe (b) Two-lobe (c) Three-lobe

Fig. 1 Sinusoidal models of acceleration pulse

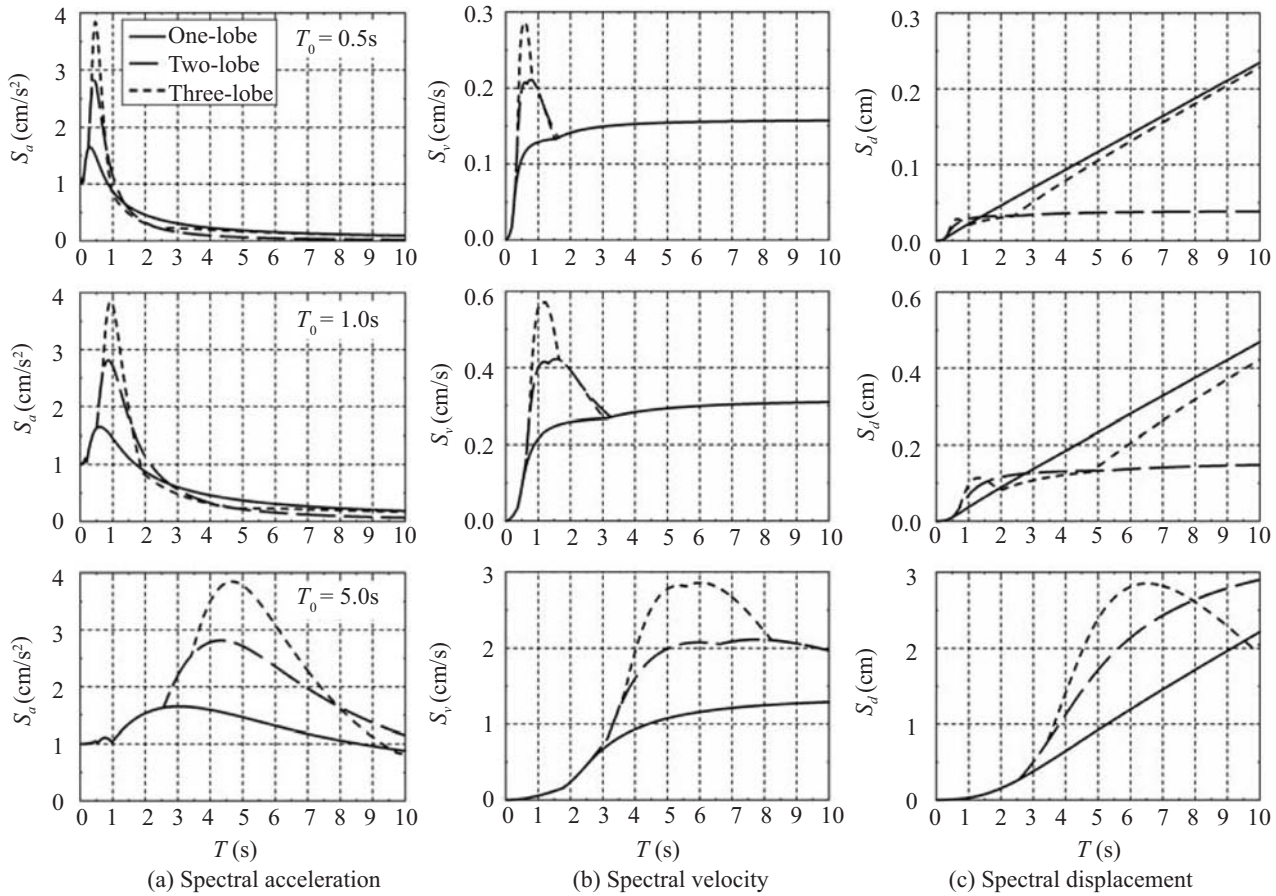

Fig. 2 Spectral accelerations, velocities, and displacements of the one-, two- and three-lobe sinusoidal acceleration pulses with T_0 being 0.5s, 1.0s, and 5.0s, respectively (damping ratio $\zeta = 0.05$)

practical engineering structures.

Spectral accelerations exhibit the following features:

(1) In the resonance band, the more lobes the input pulse contains, the larger the corresponding spectral acceleration, since it takes longer time for resonance to build up as the number of lobes increases.

(2) The predominant periods, where the spectral accelerations reach their maximum values, occur in the resonance band and with an increase in the number of lobes, they become closer to the input sinusoidal pulse periods, T_0, which is also caused by the increasing time for resonance to build-up with the increment of the lobe number. This observation suggests that the input acceleration pulse imposes much higher base shear demands on resonance-band structures than non-resonance-band structures.

(3) In the non-resonance band, the spectral accelerations become very small and are less dependent on the number of lobes contained in the input pulses.

(4) For pulses with the same number of lobes, as the value of T_0 increases, the maximum spectral accelerations are almost of the same order, but the resonance band becomes longer, which means that the longer the period of the input pulse, the more the structure is influenced by the pulse. In this sense, the resonance band can be also viewed as the influence band, where the acceleration pulse imposes severe base shear demands on a structure whose natural period falls in the band, and with the increment of the lobe number, these demands also increase.

The following observations are made for spectral velocities:

(1) In the resonance band, the variations of spectral velocities with the number of lobes contained in the input pulses and the mechanism embedded in such variations are the same as those of the spectral accelerations.

(2) For two-lobe and three-lobe input pulses, the predominant periods, where the spectral velocities reach their maximum values, are in the resonance band; while for one-lobe input pulses, the predominant period is in the non-resonance band.

(3) In the non-resonance band, the spectral velocities of one-, two-, and three-lobe pulses are identical and stay at a relatively high level, as compared with the spectral accelerations.

(4) As the value of T_0 increases, unlike the spectral accelerations, the maximum spectral velocities in the range of 0.0 s $\leq T \leq$ 10.0 s also increase, whereas the resonance bands still becomes wider, just like the spectral accelerations.

For spectral displacements, the following features

are observed.

(1) In the resonance band, the changes of spectral displacements are similar to the spectral accelerations and spectral velocities.

(2) As mentioned by Jennings (2001), the spectral displacements reach their maximum values in the non-resonance band instead of the resonance band, which means that the input acceleration pulses impose higher deformation demands on the long-period structures than on short-period structures.

(3) In the non-resonance band, the spectral displacements or deformation demands of one-lobe and three-lobe input pulses increase almost linearly as the natural period increases, and at very long periods, they tend to be identical, with the one-lobe spectral values being higher than the three-lobe; while for two-lobe input pulses, as the natural period increases, the spectral displacement tends to be a constant, whose value has been formulated by Jennings (2001).

(4) Different from the spectral accelerations but similar to the spectral velocities, the maximum spectral displacements increase as this input pulse period, T_0, increases, in the range of $0.0\ \text{s} \le T \le 10.0\ \text{s}$.

From the above discussion, it is seen that with the amplitude being equal, the acceleration pulse with a longer period would not only affect more engineering structures, i.e., induce high base shears in more structures, but also impose more severe deformation demands on structures with moderate or long periods. Such properties of the simplified acceleration pulses disscussed are like those of the near-fault ground motions with forward directivity or fling step effects, which contain distinct velocity pulses and have special yet severe damage potential to engineered structures. Like the acceleration pulses with comparatively long periods, these near-fault ground motions generally impose high base shear demands on more structures as well as severe deformation demands on long-period structures (Malhotra, 1999). As an example, the damage that the Olive View Hospital sustained during the 1971 San Fernando, California earthquake was attributed to the effect of the impulsive near-fault ground motions on flexible structures (Bertero *et al*., 1978). This might be due to the pulse natures of near-fault ground acceleration motions, which will be discussed in detail in the next section.

Finally, it should be mentioned that the discussion of general properties of the response of a structure to sinusoidal acceleration pulses is only intended to simplify the analysis in subsequent sections. In addition to the acceleration pulses modeled herein by sinusoidal pulses, there are several other mathematical approximations that may also be used to represent the realistic acceleration pulses, such as the rectangle and the triangle pulses, etc. For more detailed information about the spectral characteristics of the acceleration pulse or harmonic waves, readers may refer to Jennings (2001) or Xu *et al.* (2005).

3 Identification of near-fault acceleration pulses by EMD

After discussing the general dynamic characteristics of simplified sinusoidal acceleration pulses within the context of elastic response spectra, in this section, the acceleration pulses are identified in the near-fault acceleration records using the EMD method, and then the resulting acceleration pulses are simulated by these simplified models.

Figure 3 shows the NS components of ground motion recorded at the TCU052 station during the September 20, 1999 Chi-Chi earthquake. The large LF velocity pulse can be clearly detected at the beginning of the velocity waveform, with a HF velocity pulse riding on it before the time instant of 20.0 s. The HF velocity pulse is associated with the conspicuous large-amplitude HF acceleration pulse at the same time instant in the acceleration, while the LF velocity pulse cannot

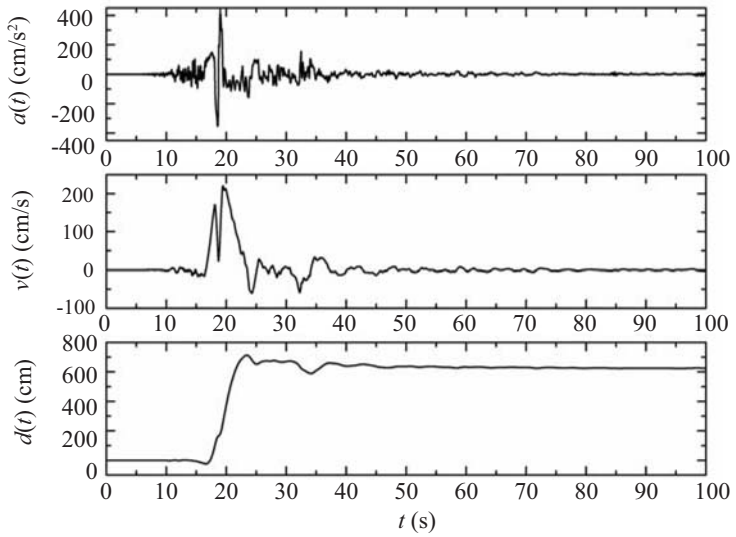

Fig. 3 NS components of ground motion recorded at the TCU052 station during the September 20, 1999 Chi-Chi earthquake

easily find its counterpart in the acceleration waveform. However, the large permanent displacement (about 6.2 m) was mainly contributed by the LF velocity pulse.

By using EMD, the velocity time history, $v(t)$, is decomposed into 10 IMFs, i.e. $c_1(t)$ to $c_{10}(t)$, as shown in Fig. 4. Adding the first three IMF components shown in Fig.4 gives the HF component of $v(t)$, i.e., the $v_1(t)$ shown in Fig.5; while adding the remaining seven IMF components yields the LF component of $v(t)$, i.e., the $v_2(t)$ shown in Fig.5. Note that the choice of the number of IMF components for the EMD-based HF and LF components is as subjective as the selection of the cutoff frequency in the Fourier-based filters (Zhang *et al*., 2003). Differentiating $v_1(t)$ and $v_2(t)$ yields the corresponding HF and LF acceleration components, $a_1(t)$ and $a_2(t)$; while integrating $v_1(t)$ and $v_2(t)$ yields the corresponding HF and LF displacement components, $d_1(t)$ and $d_2(t)$, all shown in Fig.5. In the waveform of $a_1(t)$, the HF acceleration pulse with high amplitude can be easily detected, which is associated with the HF velocity pulse before 20.0 s, but contributes little to the large permanent displacement, since the maximum value of $d_1(t)$ is only below 30.0 cm. While in the LF acceleration component, $a_2(t)$, the LF acceleration pulse associated with the large LF velocity pulse can also be easily detected, and it is this LF acceleration pulse that mainly induces the large permanent displacement about 6.2 m. Comparisons between the original waveforms and their HF and LF components are shown in Fig.6. It can be seen that the HF components (HFC) represent the details in the original waveforms, while the LF components (LFC) are the approximations of the original waveforms, with the HF components riding on the LFs to comprise the original waveforms.

The spectral accelerations, velocities, and displacements of $a(t)$, $a_1(t)$, and $a_2(t)$ are shown in Fig.7. It is seen that before the natural period of about 4.0 s, it is mainly the HF component (HFC) that dominates the structural responses; while after 4.0 s, it is the LF component (LFC) that controls the structural responses. The large deformation demands imposed by this near-fault ground motion on the long-period structures are mainly due to the LF component, while the high base shear demands with natural periods less than 4.0 s are mainly caused by the HF component.

In order to reveal the pulse natures of $a_1(t)$ and $a_2(t)$, the HF and LF acceleration pulses are isolated out of the waveforms of $a_1(t)$ and $a_2(t)$, respectively, and then the simplified sinusoidal pulses are used to model them. The isolated HF and LF acceleration pulses, $a_{1,p1}(t)$ and $a_{2,p1}(t)$, their two-lobe sinusoidal approximations, $a_{1,p2}(t)$ and $a_{2,p2}(t)$, together with $a_1(t)$ and $a_2(t)$, are shown in Fig.8. The parameters of the two-lobe sinusoidal pulses are calculated by identifying the pulse period, T_0, of, and calculating the area, S, under, the isolated acceleration pulse. Then the amplitudes of the two-lobe sinusoidal pulse, $a_{1,p2}(t)$ or $a_{2,p2}(t)$, are determined as:

$$a_0 = \frac{\pi S}{2T_0} \tag{1}$$

The values of T_0, S, and a_0 are all shown in Fig.8.

The response spectra of the HF component and its two pulse approximations are shown in the upper part of Fig.9. The spectral accelerations of $a_1(t)$, $a_{1,p1}(t)$, and $a_{1,p2}(t)$ are close to each other in the natural period range from 0.0 s to 10.0 s, which encompasses a majority of engineering structures. While their spectral velocities are close to each other in the natural period range from 0.0s to about 4.0 s, their spectral displacements are close to each other only in the range from 0.0 s to about 2.0 s. In the remaining natural period ranges, the spectral

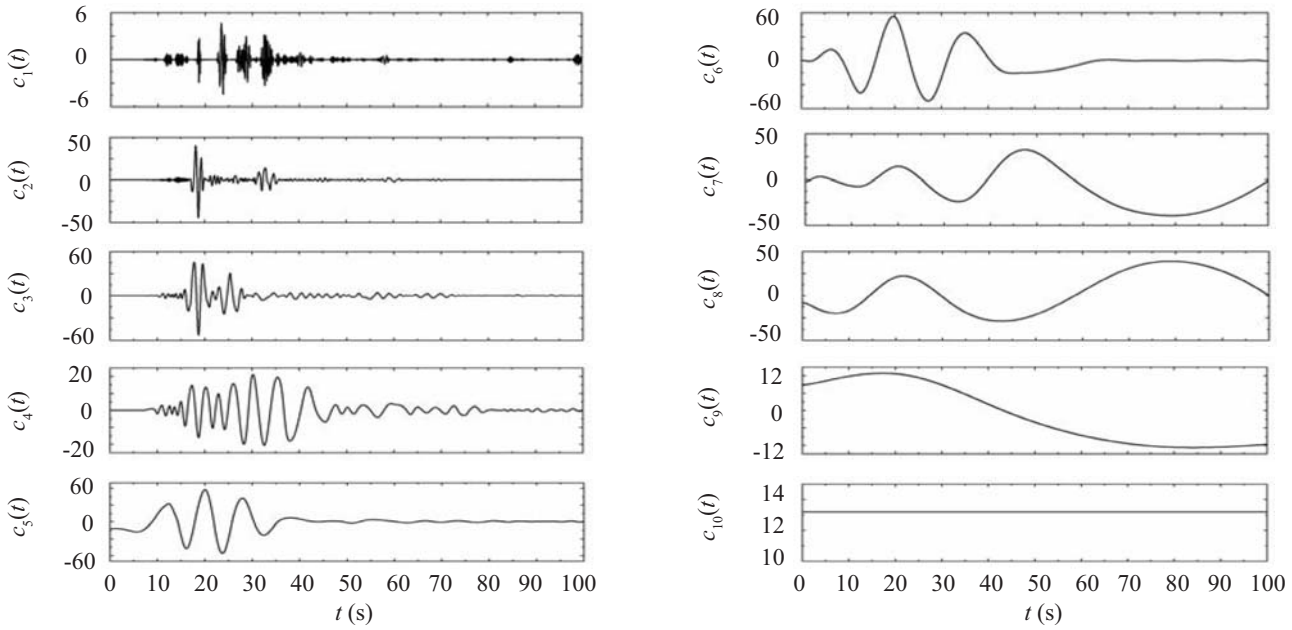

Fig. 4 IMF components of velocity time history shown in Fig. 3

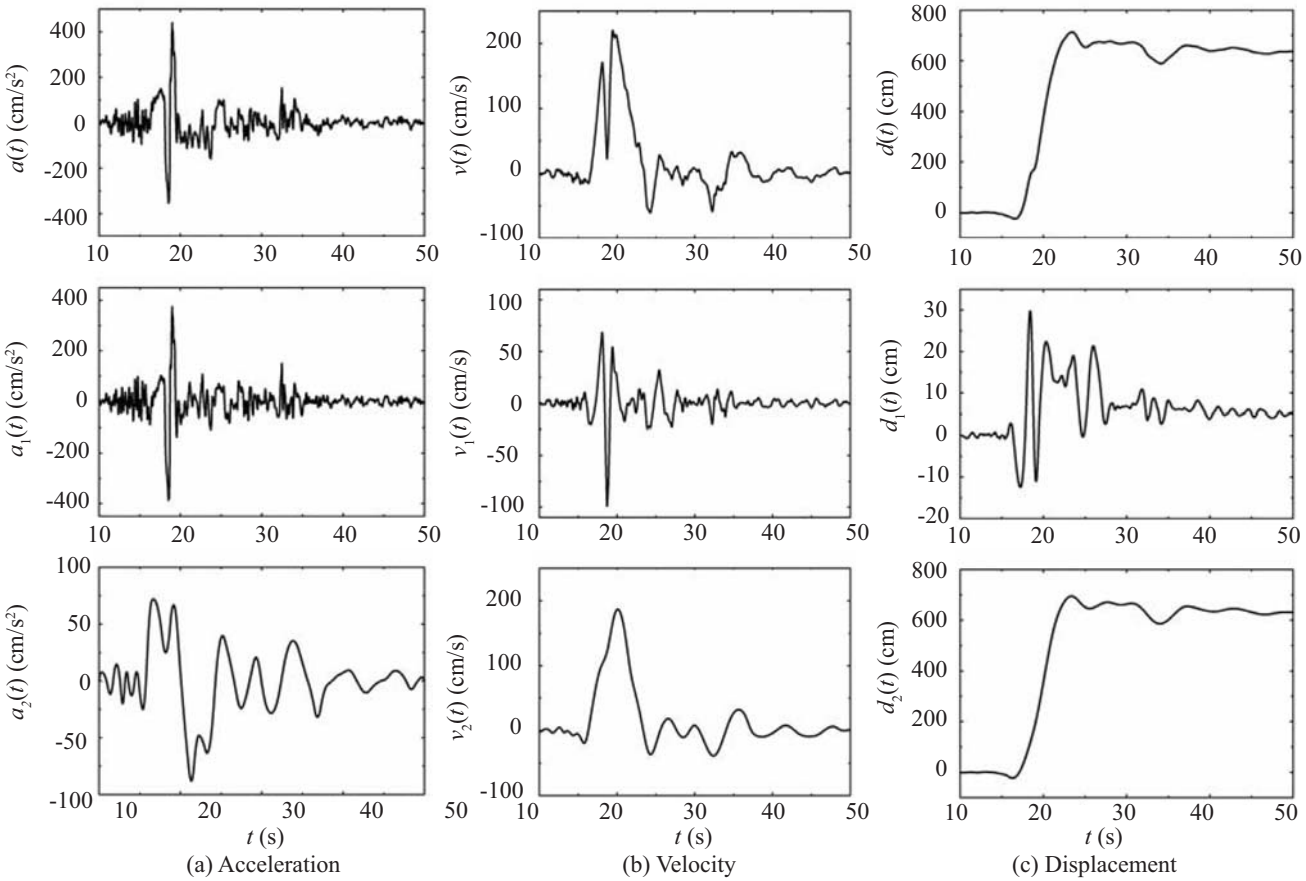

Fig. 5 The original acceleration, velocity, and displacement time histories (the upper) along with their high-frequency (HF) (the mid) and low-frequency (LF) (the lower) components (NS component, TCU052)

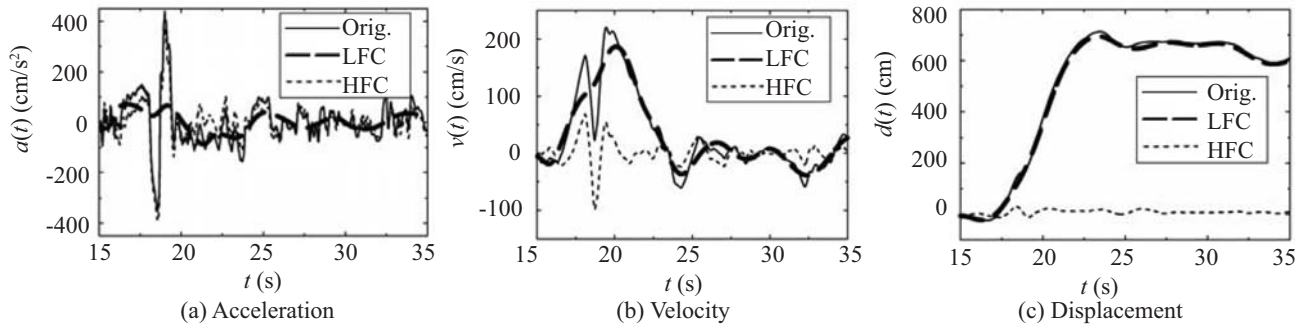

Fig. 6 Comparisons of original time histories and their LF and HF components (NS component, TCU052)

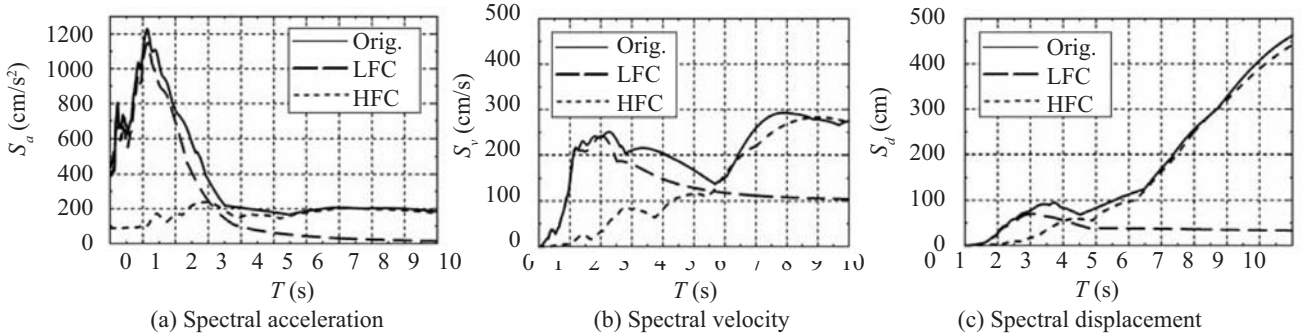

Fig. 7 Response spectra of original record and its LF and HF components (NS component, TCU052; $\zeta = 0.05$)

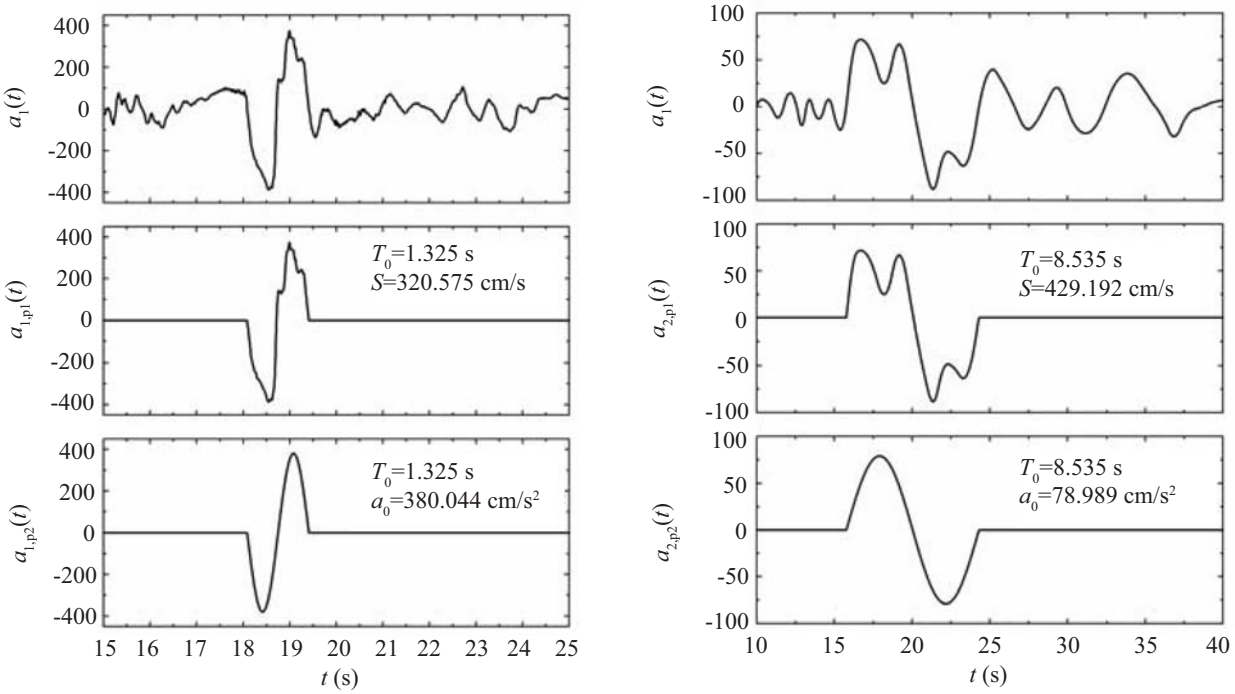

(a) HF component and its pulse approximations (b) LF component and its pulse approximations

Fig. 8 The HF, LF components and their pulse approximations (NS component, TCU052)

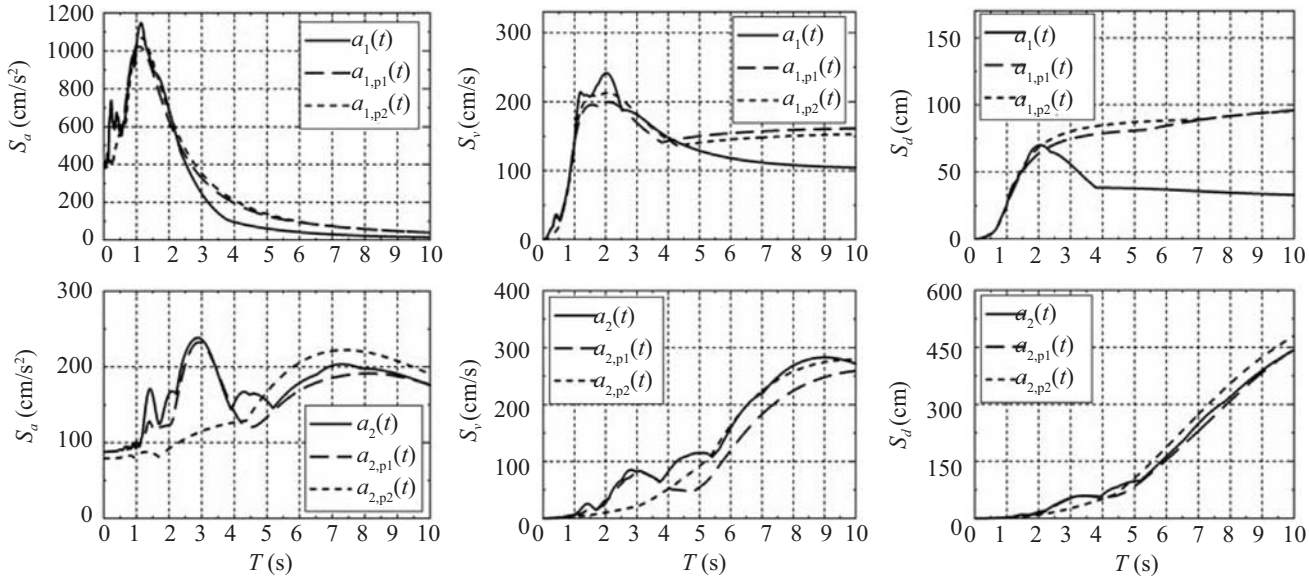

(a) Spectral acceleration (b) Spectral velocity (c) Spectral displacement

Fig. 9 Response spectra of HF, LF components and their pulse approximations (NS component, TCU052; ζ = 0.05)

values of $a_{1,p1}(t)$ and $a_{1,p2}(t)$ are consistent but higher than those of $a_1(t)$. Such discrepancies are caused by the remaining motion in $a_1(t)$ after the HF acceleration pulse with high amplitude is extracted from $a_1(t)$, i.e., the motion of $a_1(t)$-$a_{1,p1}(t)$. Even so, the similarities among the response spectra of $a_1(t)$, $a_{1,p1}(t)$, and $a_{1,p2}(t)$ still demonstrate that it is the high-amplitude acceleration pulse in the HF component, $a_1(t)$, that dominates the dynamic responses of most short-period and moderate-long-period structures. Further, the simple yet effective sinusoidal pulse models this HF acceleration pulse very well.

Note that the duration of the HF acceleration pulse is 1.325 s, which is significantly long, as described in the preceding section. The resonance band of this pulse is from the natural period of 0.0 s (rigid body) to about 4.0 s, which is where the vibration periods of most engineered structures fall. Thus, it is just this HF acceleration pulse that causes the original ground motion to impose high base shear demands on structures whose

natural vibration period range is much wider than that of the structures excited by the normal far-field ground motions (Malhotra, 1999), as is seen in the spectral accelerations in Figs.7 and 9. However, because the HF acceleration pulse has two lobes, with its period, T_0, being not long enough, the deformation demands it may impose on long-period structures is not very severe.

The response spectra of the LF component and its two pulse approximations are shown in the lower part of Fig. 9. It can be seen that the spectral velocities and displacements of $a_2(t)$, $a_{2,p1}(t)$, and $a_{2,p2}(t)$ are close to one another for most engineering structures, and in the very-long-period range from about 4.0 s to 10.0 s, their spectral accelerations are also close to one another. However, in the band from 0.0 s to 4.0 s, the spectral accelerations of $a_2(t)$ and $a_{2,p1}(t)$ are close to each other but higher than the sinusoidal approximation, $a_{2,p2}(t)$. This is due to the fact that in this band, the LF acceleration pulse with its T_0 being about 8.535 s should be regarded as a very slow pulse, whose details remarkably influence the structural dynamic responses. Even so, the observation that the spectral accelerations, velocities, and displacements of $a_2(t)$ and $a_{2,p1}(t)$ are close to each other still validates that the LF acceleration pulse of $a_{2,p1}(t)$ controls the dynamic responses of most structures when excited by the LF component, $a_2(t)$. The sinusoidal pulse models this LF acceleration pulse well in the long-period range.

The duration of the LF acceleration pulse is 8.535 s, which is so long that the normal structural natural period range from 0.0 s to 10.0 s is still in the resonance band of the pulse. Thus, when excited by it, the dynamic responses of almost all practical engineering structures would be amplified due to the build-up of resonance. However, as can be seen from the spectral accelerations, the base shear demands imposed by this LF acceleration pulse are not so severe as the HF one, which is due to the lower amplitude of the LF acceleration pulse, being only about 80 Gal, as compared with 380 Gal of the HF acceleration pulse. If the spectral acceleration were divided by the maximum amplitude of the corresponding input acceleration pulse, then the normalized spectra, or the amplification factor spectra, of the HF and LF acceleration pulses would be of the same levels, with the influence band, i.e. the natural period range where the amplification factor is larger than unit, of LF acceleration pulse being wider. On the other hand, in spite of its lower amplitude, this LF acceleration imposes much higher deformation demands on structures with moderate or long periods than the HF acceleration, as can be seen in Fig. 9(c). Further, it is only this LF acceleration pulse that engenders the original ground motion in Fig.3 to generate severe deformation demands on long-period structures, as is seen from the spectral displacements in Figs. 7 and 9.

In this example, the acceleration recording contains both the HF and the LF acceleration pulses. Generally speaking, a near-fault pulse-like ground motion contains long-period velocity pulses, which result in the LF acceleration pulse. That is to say, the near-fault pulse-like ground motion usually contains the LF acceleration pulse, but it does not necessarily contain the HF acceleration pulse like the one in this example. To make this phenomena more clear, consider the following example.

Figure 10 shows the EW components of ground motion recorded at the TCU075 station during the September 20, 1999, Chi-Chi, earthquake. It can be seen that there is no distinct large HF acceleration pulse contained in the acceleration time history, $a(t)$. Nonetheless, there is a large velocity pulse at the beginning of the velocity history, which is associated with the large permanent displacement. When processed by EMD, the velocity history, $v(t)$, is decomposed into ten IMFs, as shown in Fig.11. Similarly, adding the first three and the remaining seven IMF components provides the HF and LF velocity components, i.e. $v_1(t)$

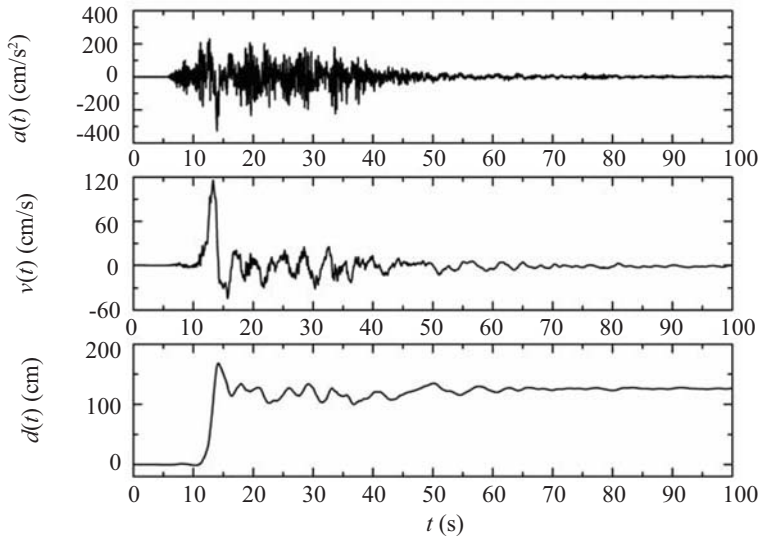

Fig. 10 EW components of ground motion recorded at TCU075 station during the September 20, 1999, Chi-Chi earthquake

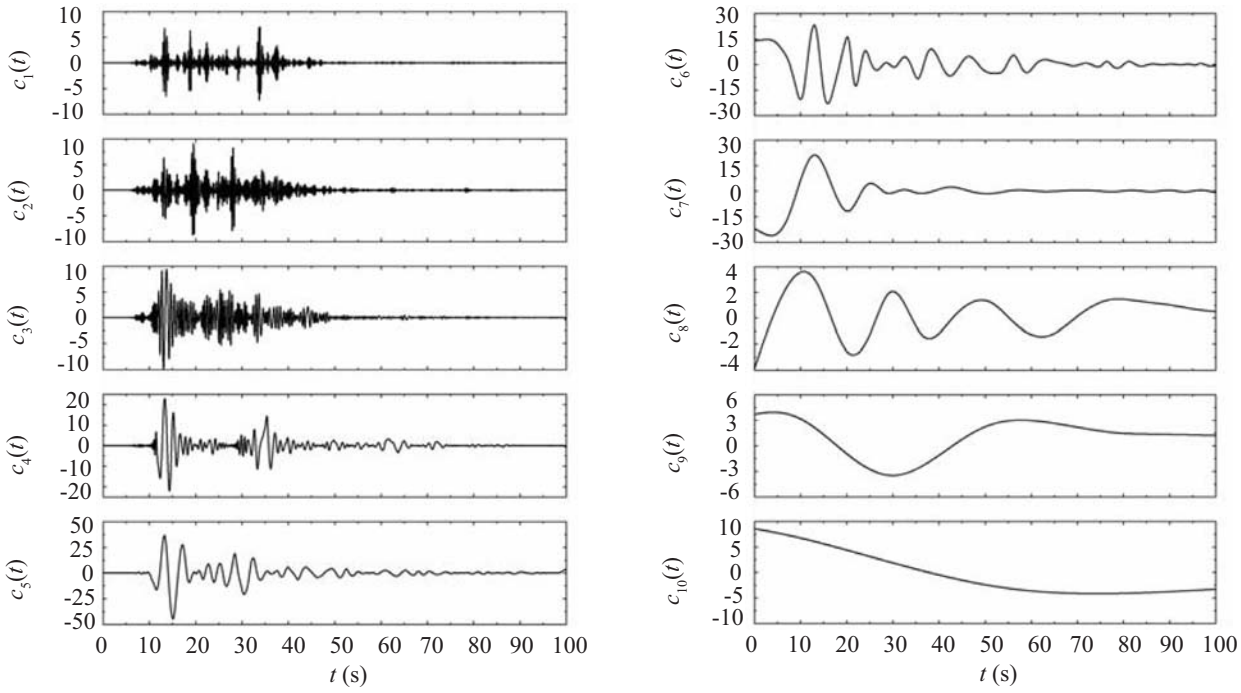

Fig. 11 IMF components of velocity time history shown in Fig.10

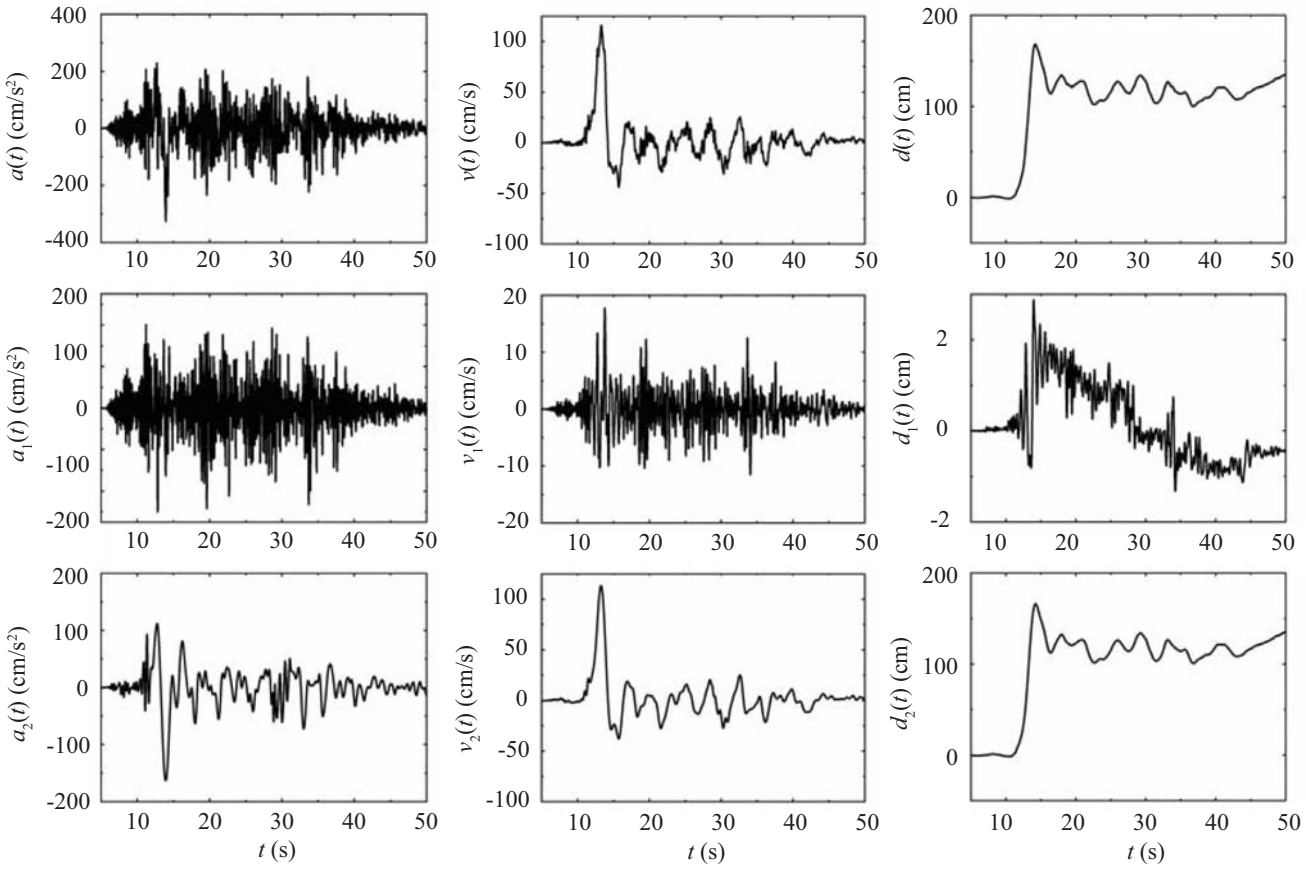

(a) Acceleration (b) Velocity (c) Displacement

Fig. 12 Original acceleration, velocity, and displacement time histories with their corresponding high-frequency (HF) and low-frequency (LF) components (EW component, TCU075)

and $v_2(t)$ in Fig.12(b), respectively. Differentiating and integrating $v_1(t)$ and $v_2(t)$ yield the corresponding HF and LF acceleration components, $a_1(t)$ and $a_2(t)$, and displacement components, $d_1(t)$ and $d_2(t)$ in Fig.12(a) and (c), respectively. It can be seen that in the HF acceleration component, $a_1(t)$, there is no distinct large-amplitude HF acceleration pulse that can be detected, and the waveform of $a_1(t)$ is like most of the ordinary far-field ground motions that are typically broad-frequency-band excitations (Chopra and Chintanapakdee, 2001). Moreover, the HF displacement, $d_1(t)$, is very small. Whereas, there is a distinct LF acceleration pulse contained in the LF component after the time instant of 10.0 s, which is associated with the large velocity pulse as well as with the large permanent displacement.

The spectral accelerations, velocities, and displacements of $a(t)$, $a_1(t)$, and $a_2(t)$, with damping ratio of 0.05, are shown in Fig.13. The figure shows that only before the natural period of about 1.0 s does the HF component (HFC), $a_1(t)$, dominate the structural responses, i.e. contribute to the high base shear demands imposed by the original motion on such short-period structures; whereas, the LF component (LFC), $a_2(t)$, controls the dynamic responses of a majority of structures, whose natural periods are larger than 1.0 s. Further, it is the LF component that imposes the high deformation demands on moderate-long- and long-period structures.

To investigate the pulse nature of the LF component, $a_2(t)$, the LF acceleration pulse is first isolated from $a_2(t)$, resulting in the time history of $a_{2,p1}(t)$ in Fig.14. The two lobes of this acceleration pulse, $a_{2,p1}(t)$, are asymmetrical in their amplitudes and periods. To model these pulses, both the asymmetrical and the symmetrical sinusoidal approximation are used. In the waveform of $a_{2,p1}(t)$, the periods of the first and second lobe are denoted by $T_{0,1}$ and $T_{0,2}$, with the corresponding areas being S_1 and S_2, respectively. When the asymmetrical approximation, $a_{2,p2}(t)$, is adopted, the amplitudes of the two successive half sinusoidal waves, $a_{0,1}$ and $a_{0,2}$, are calculated by Eq. (1), with the term S in Eq.(1) taking values of $2S_1$ and $2S_2$, respectively; while, when the symmetrical approximation, $a_{2,p3}(t)$, is adopted, the uniform period, T_0, is the average of $T_{0,1}$ and $T_{0,2}$, i.e. $T_0 = (T_{0,1}+T_{0,2})/2$, the area, S, is the sum of S_1 and S_2, i.e. $S = S_1+S_2$, and the amplitude of the sinusoidal wave, a_0, is determined by Eq. (1) accordingly. All the above values are presented in Fig.14.

The response spectra of the LF component, $a_2(t)$, together with those of its three pulse approximations, i.e., $a_{2,p1}(t)$, $a_{2,p2}(t)$, and $a_{2,p3}(t)$, are shown in Fig.15. It can be seen that the response spectra of the LF component

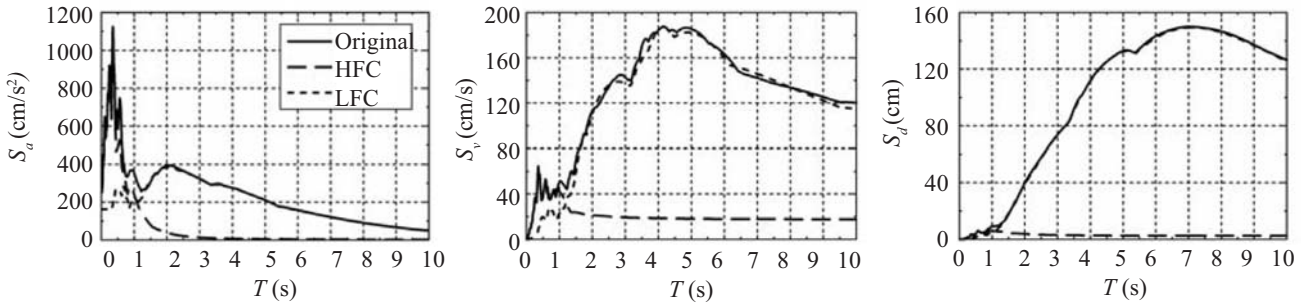

(a) Spectral acceleration (b) Spectral velocity (c) Spectral displacement

Fig. 13 Response spectra of original record and its LF and HF components (EW component, TCU075; $\zeta = 0.05$)

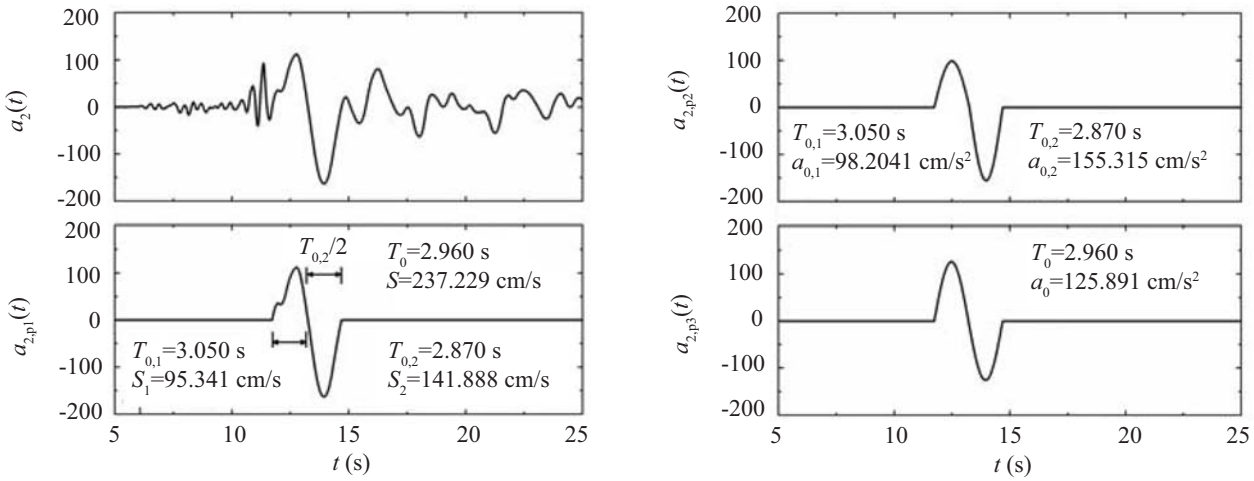

Fig. 14 LF component and its pulse approximations (EW component, TCU075)

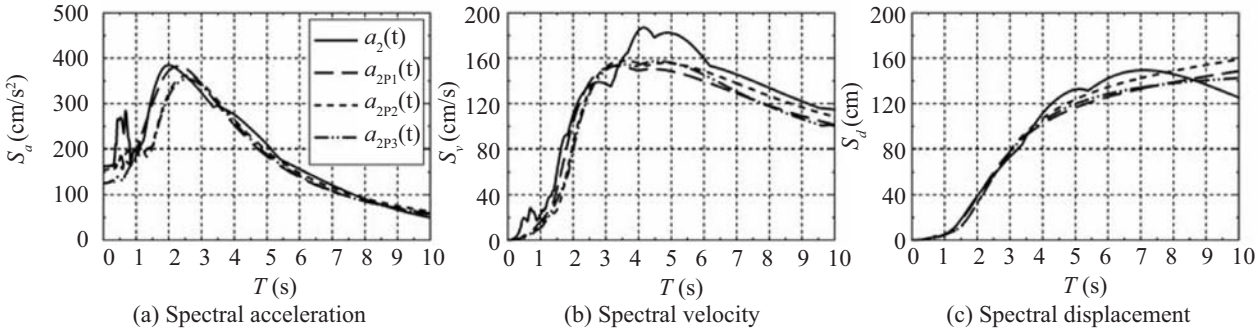

(a) Spectral acceleration (b) Spectral velocity (c) Spectral displacement

Fig. 15 Response spectra of LF component and its pulse approximations (EW component, TCU075; $\zeta = 0.05$)

and its three pulse approximations are close to one another, which demonstrates the pulse nature of this LF acceleration component: it is only the LF acceleration pulse contained in it that dominates the dynamic responses of most structures when excited by this LF acceleration component. Further, the two sinusoidal pulse models both simulate the LF acceleration pulse very well. Because the period of the LF acceleration pulse is about 2.960 s, its resonance band is from the natural period of 0.0 s up to almost 9.0 s, which means that when excited by such a pulse, the dynamic responses of most engineered structures is amplified since resonance has a finite time to accumulate. However, the duration of the acceleration pulse is only about 2.960 s, so when applied to a structure, resonance has a certain amount of time to accumulate, but does not have as much time as when subjected to the cyclic broad-frequency-band excitation of $a_1(t)$. As a result, in the predominant period band of $a_1(t)$, from 0.0 s to 1.0 s, the spectral accelerations of $a_1(t)$ are much higher than those of $a_2(t)$ and its pulse approximations, although the peak motions of $a_1(t)$, $a_2(t)$ and the pulse approximations of $a_2(t)$ are of the same levels.

In this example, unlike the preceding one, the near-fault ground motion does not contain the easily-detected HF acceleration pulse, but instead contains only the prominent velocity pulse, from which the LF acceleration pulse with a relatively long period is identified by the EMD method and modeled by simplified sinusoidal pulses. Further, it is only this LF acceleration pulse that controls the dynamic behavior of the original near-fault ground motion in the context of the elastic response spectra.

Finally, it should be added that the TCU052 and TCU075 stations are both in the near-fault region and their locations as well as the epicenter of mainshock of Chi-Chi earthquake were proposed by Loh *et al* (Loh *et al*., 2000).

4 Conclusions

In this paper, some fundamental dynamic properties of acceleration pulse are studied by using simplified sinusoidal approximations. To reveal the impulsive nature of near-fault ground motion with forward directivity or fling step effects, the empirical mode decomposition (EMD) method is adopted to identify the acceleration pulses, which are mathematically modeled by the sinusoidal pulses. The following conclusions are drawn:

(1) According to the ratio of the acceleration pulse period to the natural vibration period of the structure, the input acceleration pulse can be classified as a fast pulse or a slow pulse. Correspondingly, in the response spectra, the abscissa of the natural period can be segmented into the resonance band (or the influence band) and the non-resonance band of the input acceleration pulse.

(2) For structures with natural vibration periods falling within the resonance band, higher base shear demands are imposed by the acceleration pulse, while for structures with natural vibration periods falling in the non-resonance band, higher deformation demands are imposed. Further, in each band, the corresponding demand is controlled by the duration of, or the number of lobes contained in, the pulse. However, sometimes in the resonance band, if the acceleration pulse is a very slow pulse, the details of the pulse also influence the structural dynamic responses.

(3) Near-fault ground motion with forward directivity or fling step effects, which imposes high base shear demands on more engineered structures than broad-band far-field shaking, and also imposes severe deformation demands on long-period structures, always contains the low-frequency velocity pulse and sometimes the distinct high-frequency acceleration pulse with large amplitude.

(4) The empirical mode decomposition method (EMD) can be successfully applied to identify the LF acceleration pulse associated with the LF velocity pulse, and can separate the HF and LF acceleration pulses from the original motion if it contains the HF acceleration pulse. Further, it is just the LF acceleration pulse, together with the HF acceleration pulse if present, that dominates the special impulsive dynamic behaviors of original near-fault pulse-like ground motion and imposes a unique yet severe demand on engineered structures.

(5) The simplified sinusoidal pulse, symmetrical or asymmetrical, can be used to model the HF and LF acceleration pulses contained in the near-fault ground motion to some extent, enabling the characteristics of structural response to near-fault ground motions to be

understood.

References

Agrawal AK and He WL (2002), "A Closed-form Approximation of Near-fault Ground Motion Pulses for Flexible Structures," *Proc. 15th ASCE Engineering Mechanics Conference*, Columbia University, New York.

Aki K (1968), "Seismic Displacements Near a Fault," *J. Geophys. Res.*, **73**(16): 5359-5376.

Alavi B and Krawinkler H (2000), "Consideration of Near-fault Ground Motion Effects in Seismic Design," *Proc. 12th World Conf. on Earthquake Engng*., Auckland, New Zealand (Feb. 4) (CD-ROM).

Archuleta RJ and Hartzell SH (1981), "Effects of Fault Finiteness on Near-source Ground Motion," *Bull. Seismological Soc. Am.*, **71**(4): 939-957.

Bertero VV (1976), "Establishment of Design Earthquakes — Evaluation of Present Methods," *Proc. Int. Symp. on Earthquake Structural Engineering*, St. Louis, Vol. 1, pp.551-580.

Bertero VV, Mashin SA and Herrera RA (1978), "Aseismic Design Implications of Near-fault San Fernando Earthquake Records," *Earthquake Engng. Struct. Dyn*., **6**(1): 31-42.

Bolt BA (1983), "The Contribution of Directivity Focusing to Earthquake Intensities," *Report No. 20, U.S. Army Corps of Engineers,* Vicksburg, MS.

Chopra AK and Chintanapakdee C (2001), "Comparing Response of SDF Systems to Near-fault and Far-fault Earthquake Motions in the Context of Spectral Regions," *Earthquake Engng. Struct. Dyn*., **30:** 1769-1789.

Dai JW, Mai T, Lee GC, Qi XZ and Bai WT (2004), "Dynamic Responses Under the Excitation Pulse Sequences," *Earthquake Engng. Engng. Vib.,* **3**(2): 157-170.

Huang NE, Shen Z, Long SR, Wu MC, Shih HH, Zheng Q, Yen NC, Tung CC and Liu MH (1998), "The Empirical Mode Decomposition and Hilbert Spectrum for Nonlinear and Nonstationary Time Series Analysis," *Proc. Roy. Soc. Lond.,* **A**(454):903-995.

Iwan WD (1997), "Drift Spectrum: Measure of Demand for Earthquake Ground Motions," *J. Struct. Engng*., ASCE, **123**(4): 397-404.

Jennings PC (2001), "Ground Motion Pulses and Structural Response," *Earthquake Engineering Frontiers in the New Millennium*, Spencer & Hu (eds), Swets & Zeitlinger.

Loh CH, Lee ZK, Wu TC and Peng SY (2000), "Ground Motion Characteristics of the Chi-Chi Earthquake of 21 September 1999," *Earthquake Engng. Struct. Dyn.*, **29**: 867-897.

Makris N and Chang SP (2000), "Response of Damped Oscillators to Cycloidal Pulses," *Journal of Engineering Mechanics*, ASCE, **126**(2): 123-131.

Makris N and Black CJ (2004), "Evaluation of Peak Ground Velocity as a Good Intensity Measure for Near-source Ground Motions," *J. Struct. Engng*., ASCE **130**(9): 1032-1044.

Malhotra PK (1999), "Response of Buildings to Near-Field Pulse-like Ground Motions," *Earthquake Engng. Struct. Dyn*., **28**: 1309-1326.

Mavroedis GP and Papageorgiou AS (2003), "A Mathematical Representation of Near-fault Ground Motions," *Bull. Seismological Soc. Am*., **93**: 1099-1131.

Mavroedis GP, Dong G and Papageorgiou AS (2004), "Near-fault Ground Motions, and the Response of Elastic and Inelastic Single-degree-of-freedom (SDOF) Systems," *Earthquake Engng. Struct. Dyn.*, **33**: 1023-1049.

Sasani M and Bertero VV (2000), "Importance of Severe Pulse-type Ground Motions in Performance-based Engineering: Historical and Critical Review," *Proc. 12th World Conf. on Earthquake Engng.*, Auckland, New Zealand (Feb. 4) (CD-ROM).

Singh JP (1985), "Earthquake Ground Motions: Implications for Designing Structures and Reconciling Structural Damage," *Earthquake Spectra*, **1**(2), 239-270.

Somerville PG, Smith NF, Graves RW and Abrahamson NA (1997), "Modification of Empirical Strong Ground Motion Attenuation Relations to Include the Amplitude and Duration Effects of Rupture Directivity," S*eismological Research Letters*, **68**: 180-203.

Someville P (1998), "Development of an Improved Representation of Near-fault Ground Motions," *SMIP98 Seminar on Utilization of Strong-Motion Data* (Sept. 15), Oakland, Calif.

Sucuogly H, Erberik MA and Yucemen MS (1999), "Influence of Peak Ground Velocity on Seismic Failure Probability," *Proc. 4th Int. Conf. of the European Association for Structural Dynamics (EURO-DYN 99)*, Prague, Czech Republic.

Xu LJ, Xie LL and Hao M (2005), "On the Response Spectra to Harmonic Ground Motion," *Engineering Mechanics*, **22**(5): 7-13. (in Chinese)

Zhang RR, Ma S, Safak E and Hartzell S (2003), "Hilbert-Huang Transform Analysis of Dynamic and Earthquake Motion Recordings," *J. Struct. Engng*., ASCE, **129**(8): 861-875.